Supporting Information

Suppressing the dissolution of organic components to construct low-solubility SEI in sodium-ion batteries: the critical role of electrolyte additive TMSPi

Jiayuan Li [a, b], *Li Li* [a, b], *Hao Liu* [a, b], *Lijing Xie* [a], *Zonglin Yi* [a, *], *Fangyuan Su* [a, *]

[a] Shanxi Key Laboratory of Carbon Materials, Institute of Coal Chemistry, Chinese Academy of Sciences, Taiyuan 030001, China

[b] University of Chinese Academy of Sciences, Beijing 100049, China

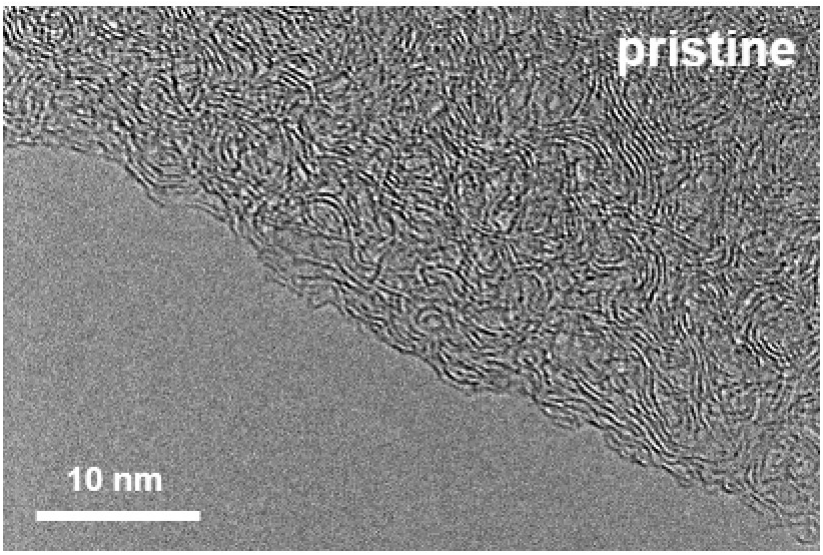

Figure S1. The TEM images of HC electrodes before cycles.

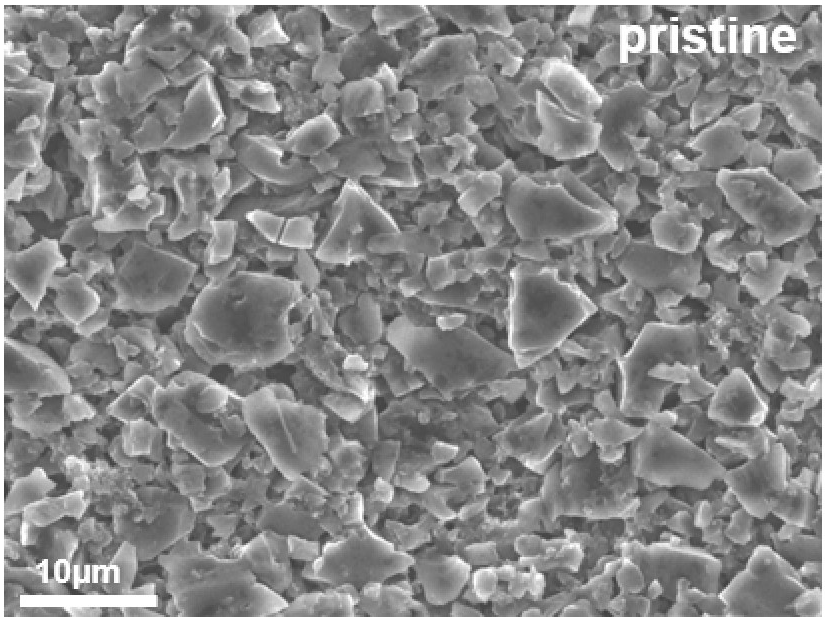

Figure S2. The SEM images of HC electrodes before cycles.

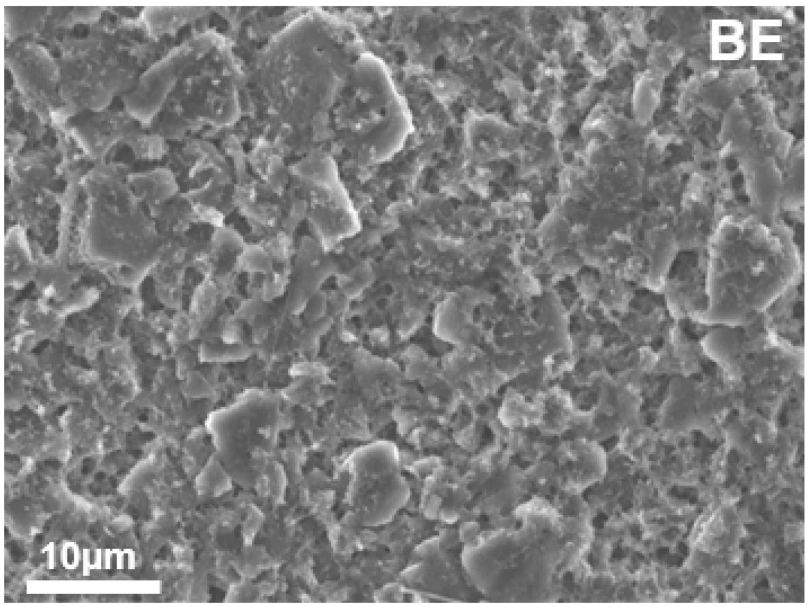

Figure S3. The SEM image of the cycled HC electrodes in Na||HC cells with BE electrolyte.

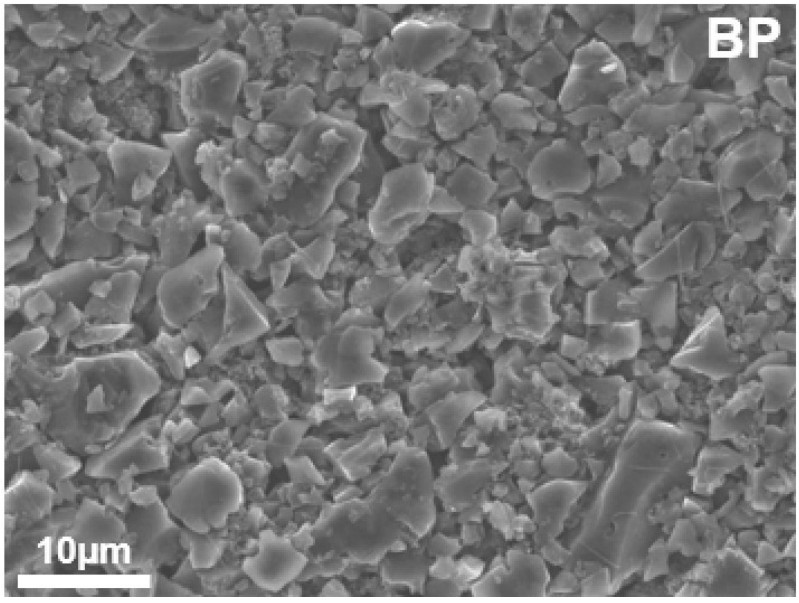

Figure S4. The SEM image of the cycled HC electrodes in Na||HC cells with BP electrolyte.

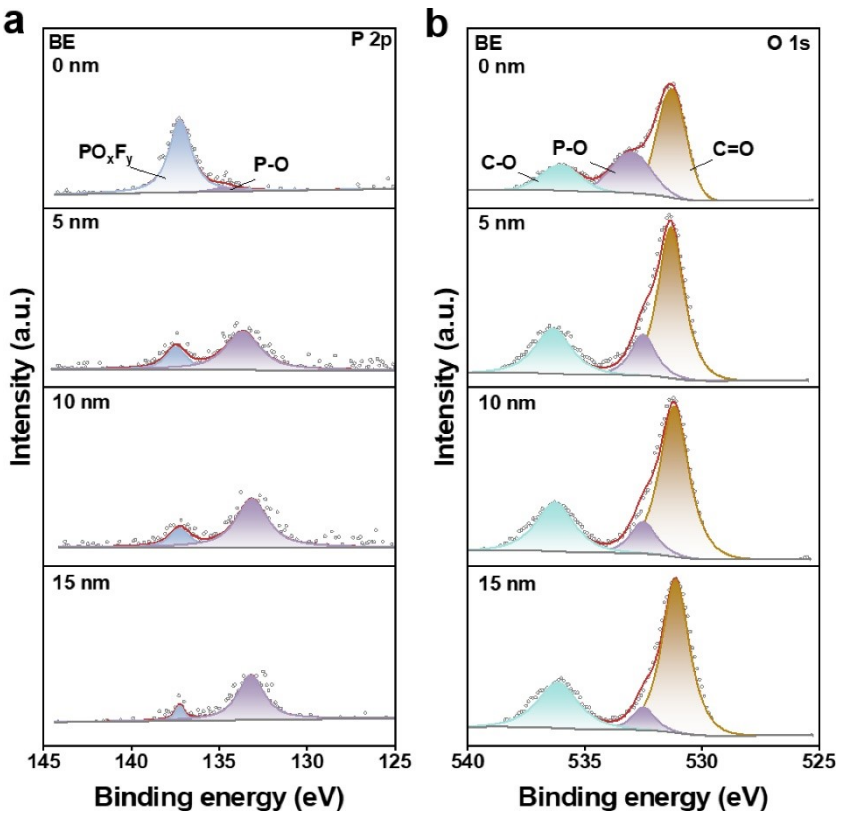

Figure S5. XPS depth spectra of (a) P 2p and (b) O 1s of the cycled HC anodes in BE electrolyte.

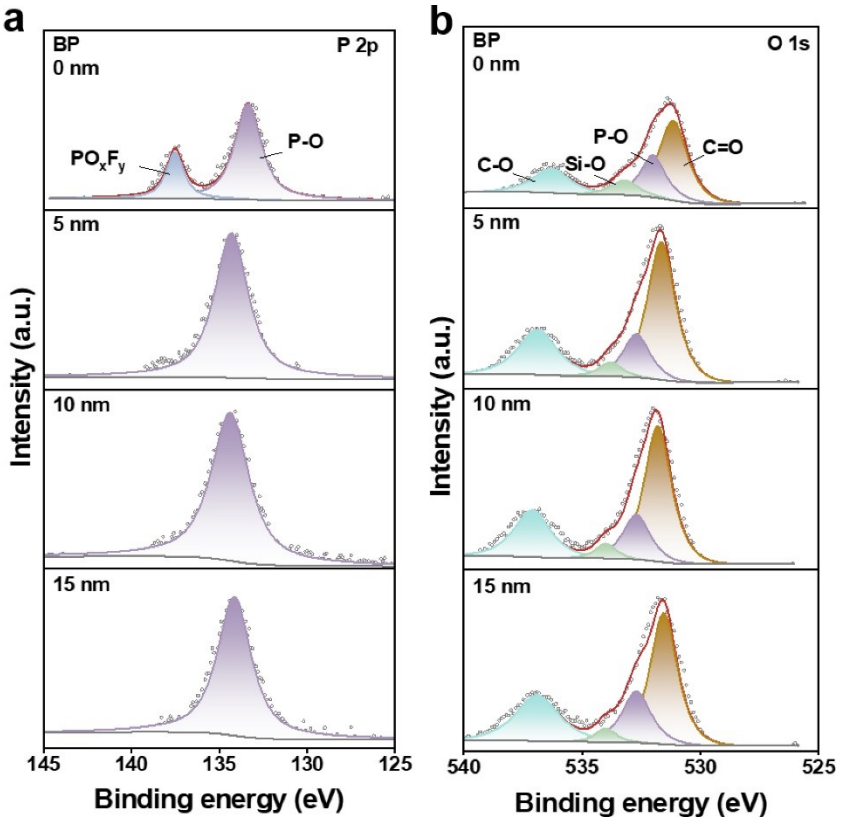

Figure S6. XPS depth spectra of (a) P 2p and (b) O 1s of the cycled HC anodes in BP electrolyte.

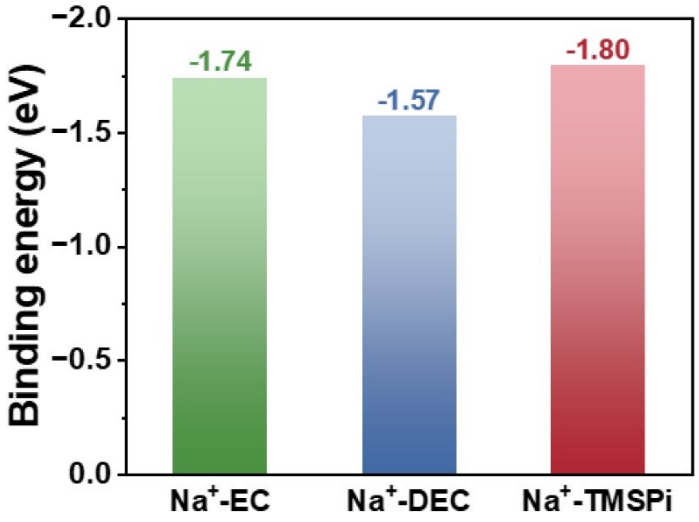

Figure S7. Binding energies of Na^+ with different solvents.

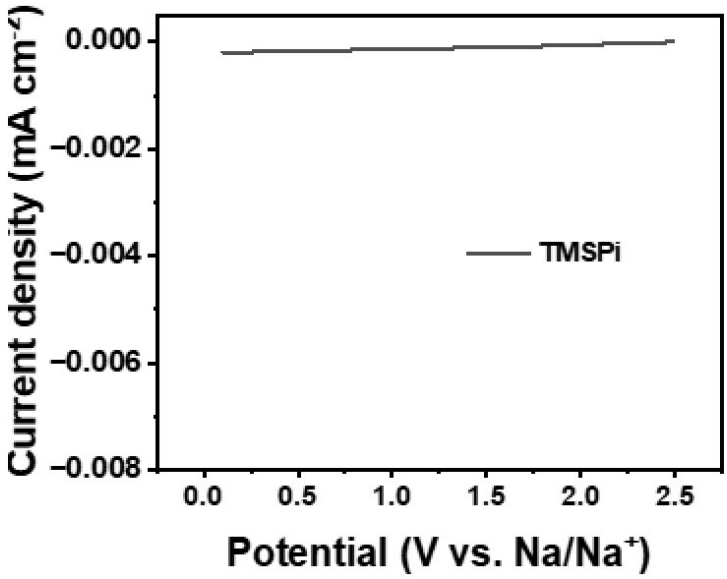

Figure S8. LSV curve of Na||Cu cell with TMSPi.

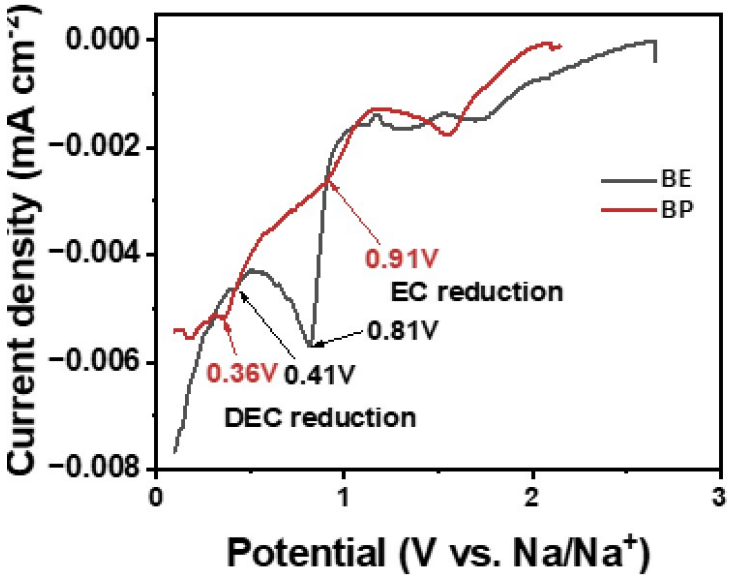

Figure S9. LSV curves of Na||Cu cells with BE and BP electrolytes.

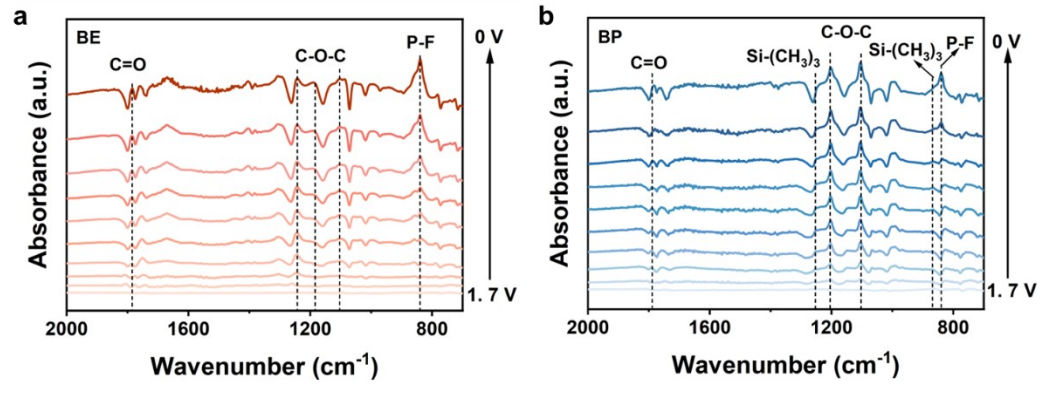

Figure S10. In situ FTIR spectra of HC anodes in (a) BE and (b) BP electrolytes.

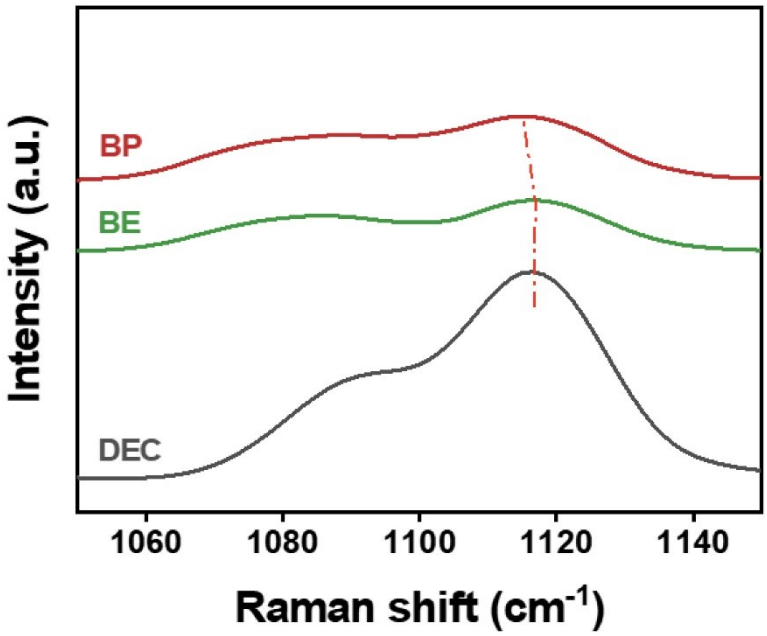

Figure S11. Raman spectra of corresponding electrolyte systems: pure DEC solvent, BE electrolyte and BP electrolyte.

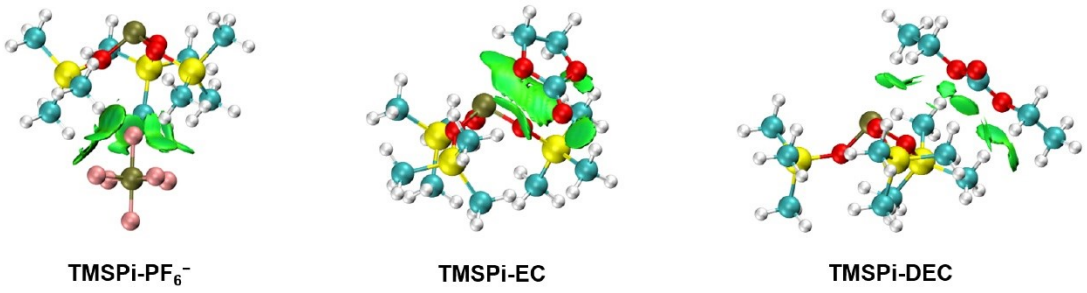

Figure S12. Interaction region indicator (IRI) diagram of TMSPi with PF_6^-, EC and

DEC molecule.

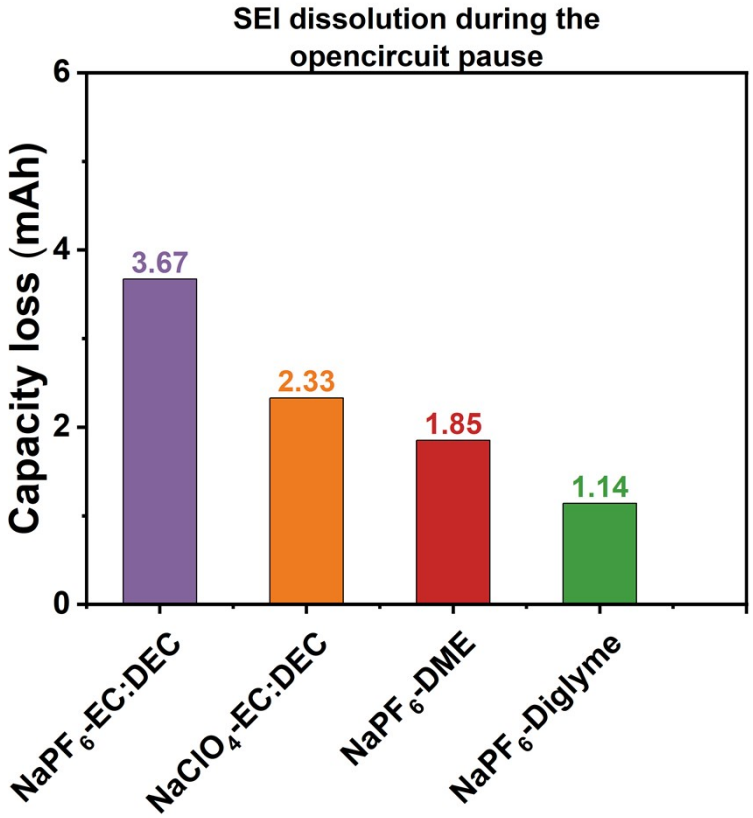

Figure S13. Absolute capacity loss after 50 h pause in each electrolyte system.

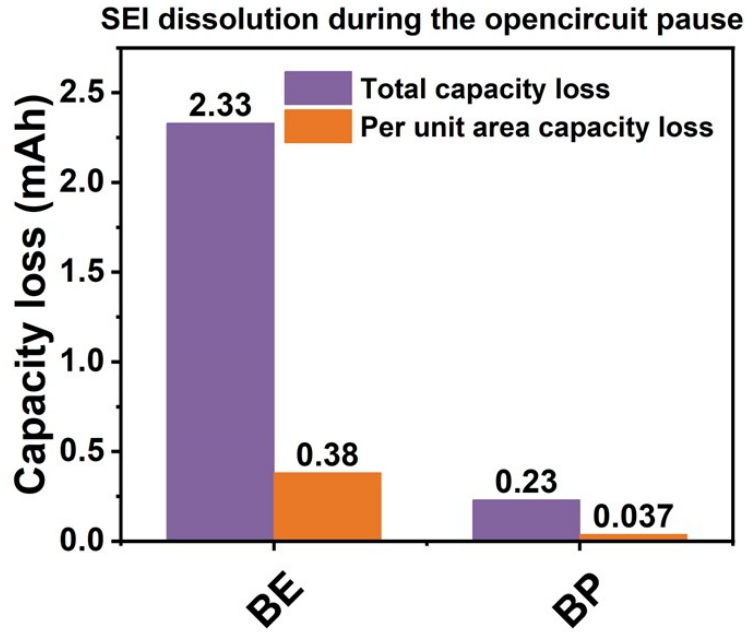

Figure S14. Absolute capacity loss after 50 h pause in BE and BP electrolytes.

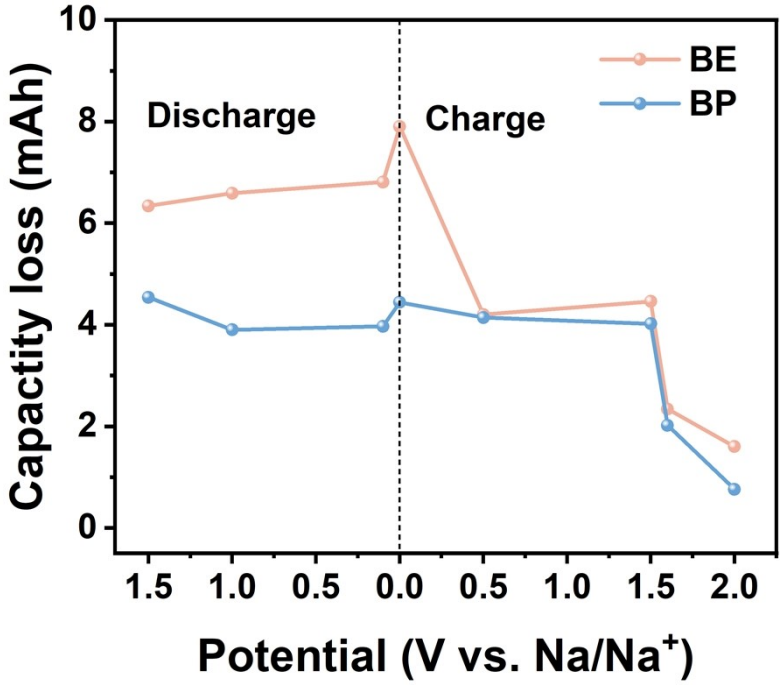

Figure S15. Dissolution capacity loss at different holding potentials.

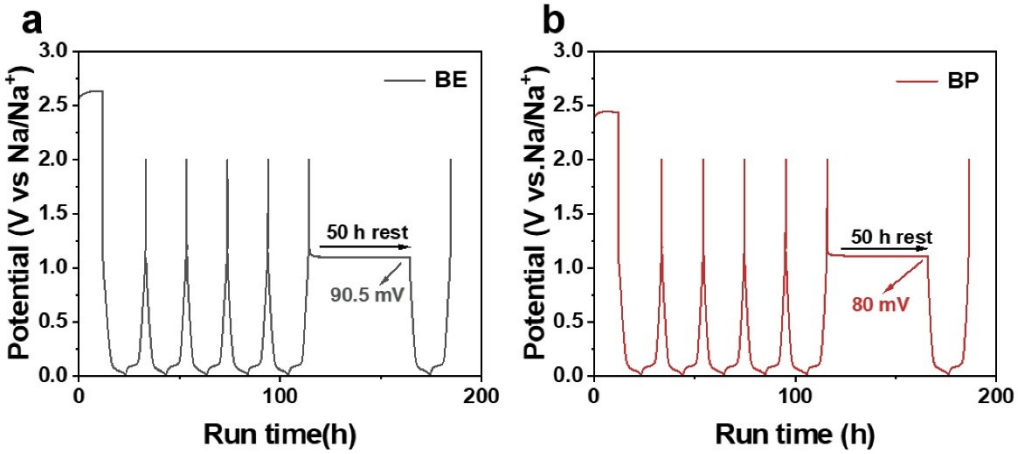

Figure S16. The voltage increases during 50 h pause of Na||HC cells with (a) BE and (b) BP electrolytes.

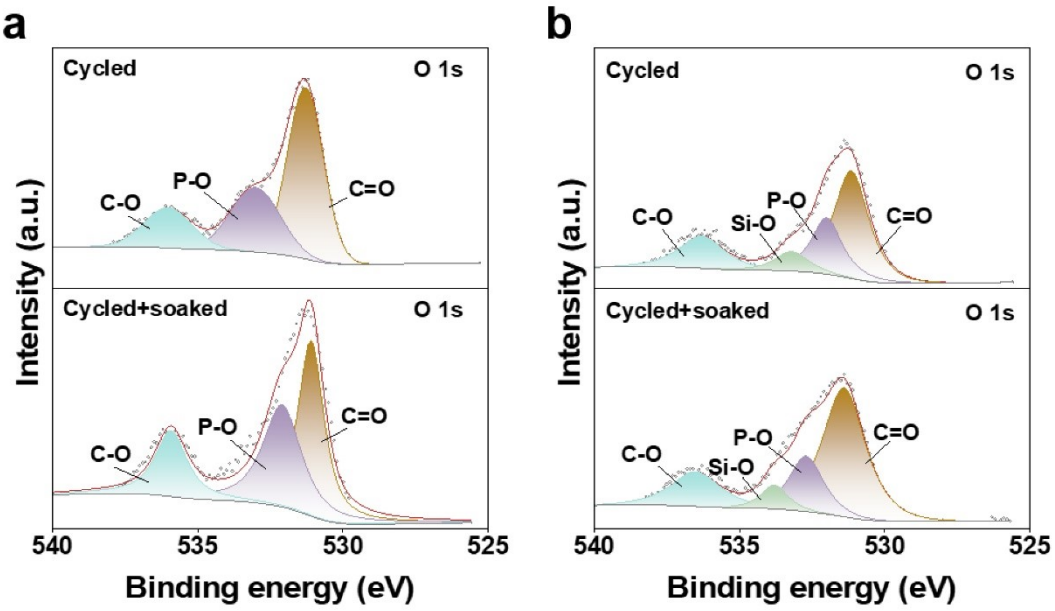

Figure S17. XPS spectra of O 1s in cycled and soaked HC electrode with (a) BE electrolyte and (b) BP electrolyte.

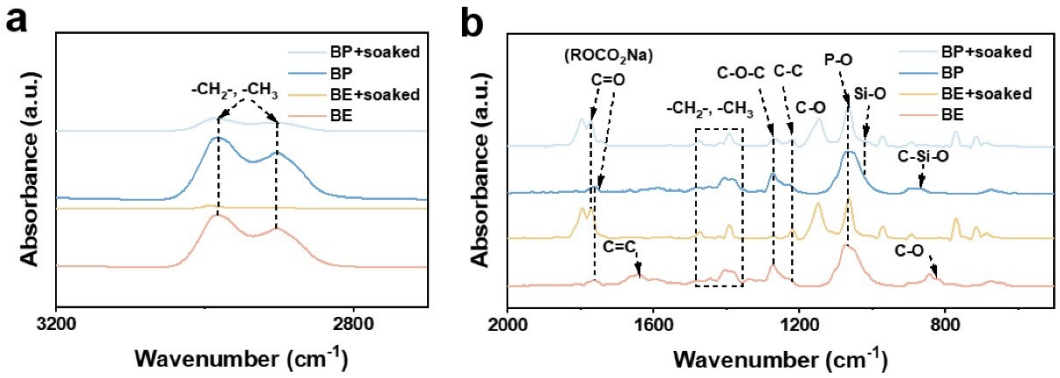

Figure S18. FTIR spectra of cycled and soaked HC anodes in BE and BP electrolytes.

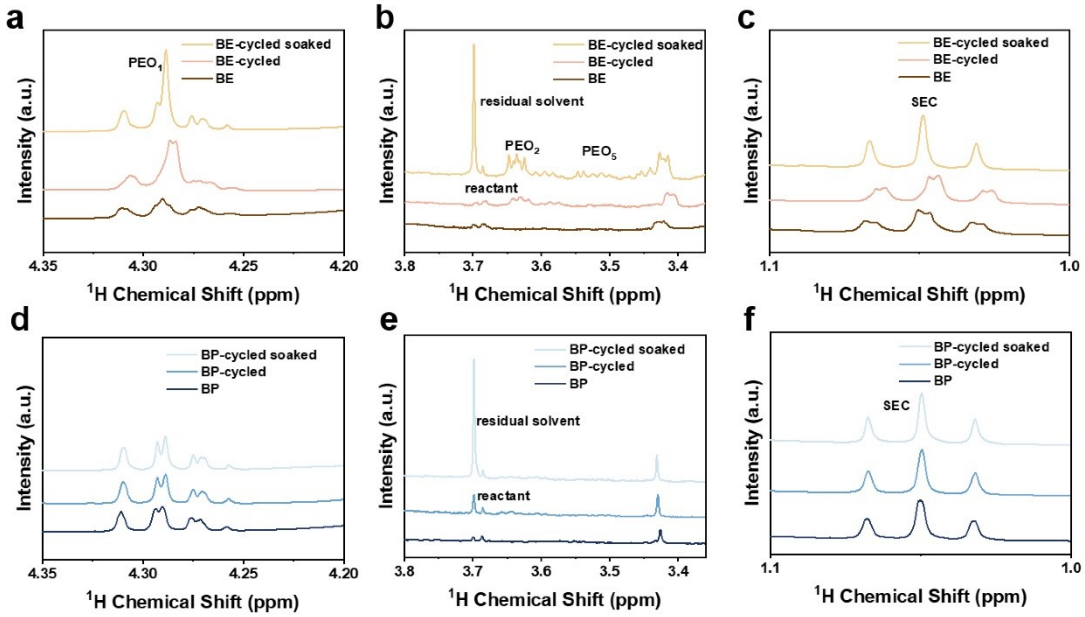

Figure S19. ^{1}H NMR spectra of SEI in (a-c) BE and (d-f) BP electrolytes before and after dissolution. The HC electrode cycled with BE and BP electrolyte were soaked in solute-free EC: DEC solvent and EC: DEC+TMSPi solvent for 50 hours, and then the solvents where the components of SEI dissolved into was compared with the cycled and uncycled electrolytes.

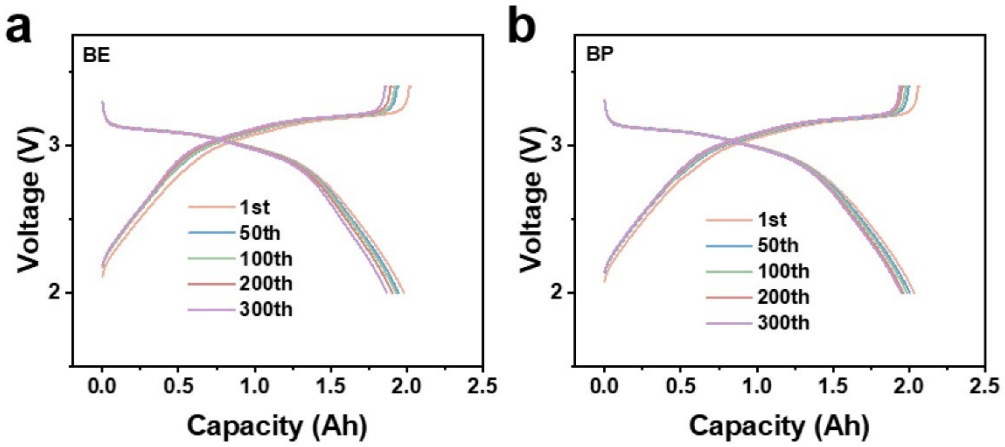

Figure S20. Voltage curves as a function of cycle number of HC||NFPP pouch cells using (a) BE and (b) BP electrolytes.

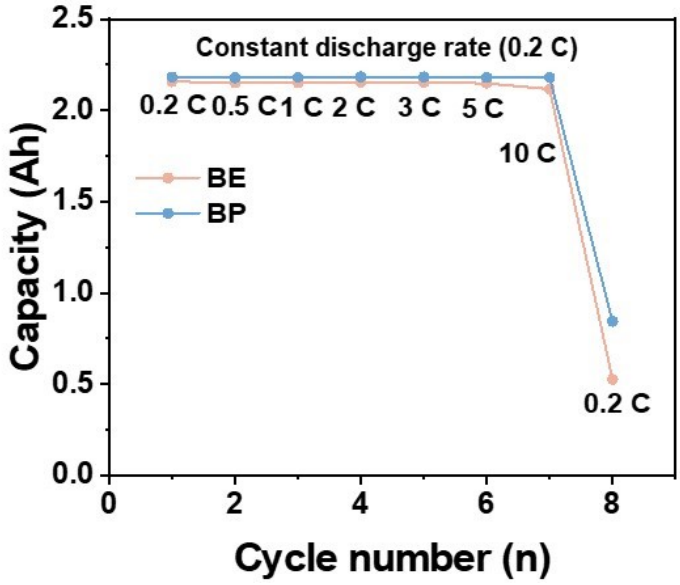

Figure S21. Rate performance of HC||NFPP pouch cells using BE and BP electrolyte

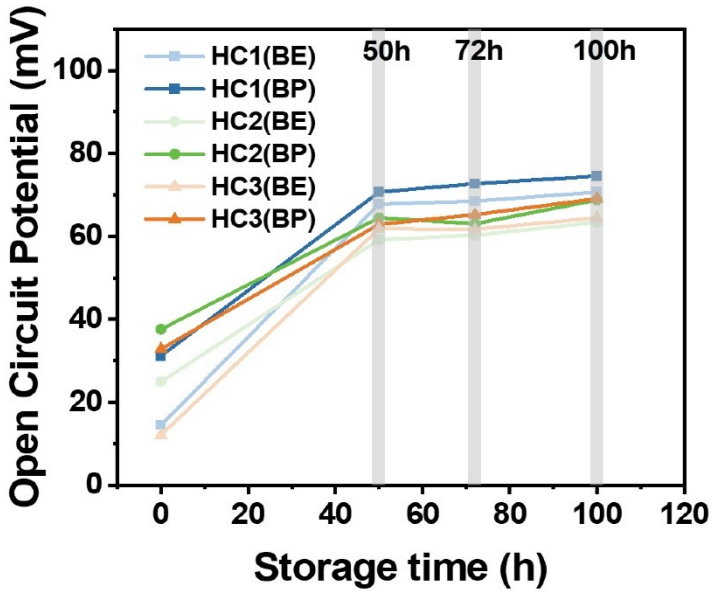

Figure S22. The summary of OCP of Na||HC cells with BE and BP electrolytes at 65 ℃.

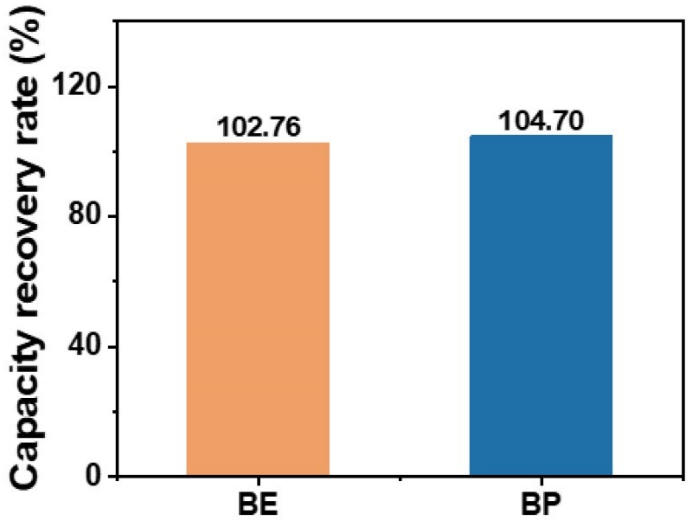

Figure S23. The capacity recovery rates of HC||NFPP pouch cells in BE and BP electrolytes at 65 ℃.

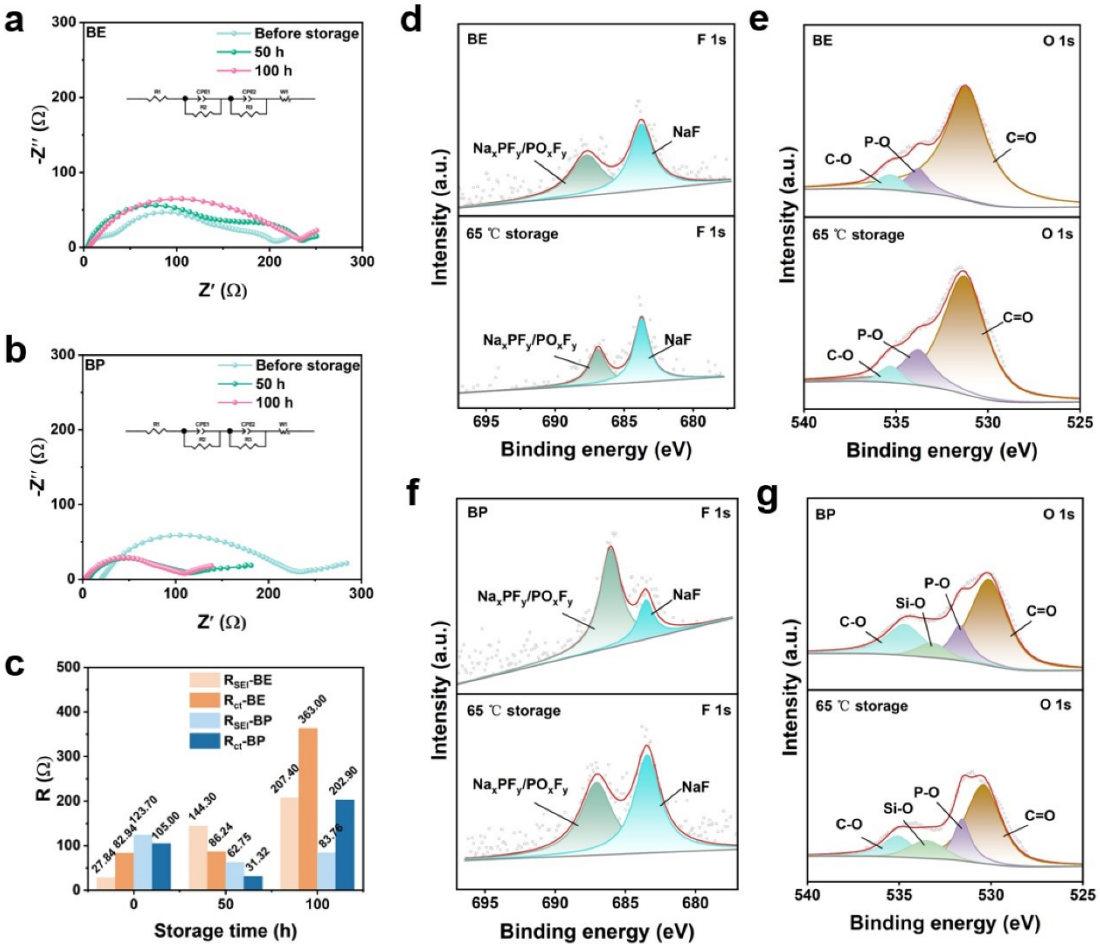

Figure S24. The EIS of Na||HC cells with (a) BE and (b) BP before storage, after storage at 65 ℃ for 50 h and 100 h. (c) The summary of Rct and RSEI after storage at 65 ℃ for 0 h, 50 h and 100 h in BE and BP. XPS spectra of (d) F 1s and (e) O 1s before and after 65 ℃ storage in BE electrolyte, (f) F 1s and (g) O 1s before and after 65 ℃ storage in BP electrolyte.

Table S1. The Cycling performance of pouch cells with different electrolytes in reference.

Cell	Electrolyte	Rate	Cycles	Capacity retention	Ref
1Ah HC||NFM	1 M $NaPF_6$ in PC: EMC: FEC (50:47:3) + 2 wt.%	0.5 C	600	84%	[1]

	DTD + 10 wt.% PFPN				
	1 M $NaPF_6$ in EC: EMC (3:7)	1 C	400/700	80%/68%	[2]
	1 M $NaPF_6$ in EC: EMC (3:7) + 3 wt.% TMSS	1 C	400/700	89%/80%	[2]
	0.8 M $NaPF_6$ in EC: EMC (3:7)	1 C	700	70%	[3]
	0.8 M $NaPF_6$ in EC: EMC (3:7) + 1 wt.% NaDFP	1 C	700	90%	[3]
	1 M $NaPF_6$ in EC: DMC (1:1) + 5% FEC	1 C	500	62%	[4]
	1 M $NaPF_6$ in EC: DMC (1:1) + 5% FEC + 1 wt.% NaDFPB	1 C	500	79%	[4]
	1 M $NaPF_6$ in EC: EMC (3:7)	0.5 C	300	39.44%	[5]
	1 M $NaPF_6$ in EC: EMC (3:7) + 2 wt.% PCS	0.5 C	300	77.56%	[5]
	1 M $NaPF_6$ in PC: EMC (1:1) + 2 vol% FEC + 2 wt.% DTD	1 C	400	87%	[6]
3Ah HC||NFM	1 M NaFSI in AN	1 C	1000	90.7%	[7]
1Ah HC||NFPP	1 M NaDFOB in G2	1 C	500	80%	[8]
	$NaClO_4$: TMP: TFEP (1:3:2)	1 C	200	84.5%	[9]

References

[1] Y. Zhang, Z. Wu, Y. Wang, G. Chen, K. Yang, L. Li, X. Liu, Z. Ma, L. Chen, Revisiting Interfacial Enhancement Effects of Fluorinated Cyclophosphaze ne in Practical Sodium-Ion Batteries, ACS Applied Materials & Interfaces 17(2 1) (2025) 31553-31560. https://doi.org/10.1021/acsami.5c02243.

[2] S. Li, H. Liu, H. Qiu, X. He, W. Fan, W. Wang, J. Nan, An electrolyte d esign strategy for commercial all-climate pouch sodium-ion batteries, Chemical Engineering Journal 505 (2025) 159102. https://doi.org/https://doi.org/10.1016/j.ce j.2024.159102.

[3] J. Cai, W. Fan, X. Li, S. Li, W. Wang, J. Liao, T. Kang, J. Nan, A dual-functional electrolyte additive for stabilizing the solid electrolyte interphase and solvation structure to enable pouch sodium ion batteries with high performance at a wide temperature range from −30 °C to 60 °C, Chemical Engineering Jour nal 491 (2024) 151949. https://doi.org/https://doi.org/10.1016/j.cej.2024.151949.

[4] R. Hu, L. Yang, C. Zhang, B. Chen, H. Hong, H. Shen, C. Mao, Z. Yang, S. Zhang, Q. Huang, Y. Li, W. Ruan, F. Yang, Bifunctional sodium tetrakis [3,5 -bis(trifluoromethyl)phenyl] borate additive for long-lifespan sodium-ion batteries with NaNi0.33Fe0.33Mn0.33O2 cathode, Chemical Engineering Journal 512 (20 25) 162144. https://doi.org/https://doi.org/10.1016/j.cej.2025.162144.

[5] J. Li, Z. Fan, H. Ye, J. Zheng, J. Qiu, H. He, P. Liu, M. He, H. Liu, N. Duc Hoa, R. Zeng, Novel sulfur-based electrolyte additive for constructing high -quality sulfur-containing electrode-electrolyte interphase films in sodium-ion batte

ries, Chemical Engineering Journal 489 (2024) 151188. https://doi.org/https://doi.org/10.1016/j.cej.2024.151188.

[6] Z. Guo, M. Yang, Q. Fan, Y. Chen, T. Xu, C. Li, Z. Li, Z. Li, Q. Sun, H. Xia, Inorganic-Enriched Solid Electrolyte Interphases: A Key to Enhance Sodium-Ion Battery Cycle Stability?, Small 20(51) (2024) 2407425. https://doi.org/https://doi.org/10.1002/smll.202407425.

[7] G. Liu, K. Zhang, Y. Cao, R. Hou, Y. Wang, X. Dong, Y. Xia, Practical and Versatile Sodium-Ion Batteries Realized With Nitrile-Based Electrolytes, Advanced Energy Materials 15(21) (2025) 2405319. https://doi.org/https://doi.org/10.1002/aenm.202405319.

[8] M. Xia, H. Chen, Z. Zheng, Q. Meng, A. Zhao, X. Chen, X. Ai, Y. Fang, Y. Cao, Sodium-Difluoro(oxalato)Borate-Based Electrolytes for Long-Term Cycle Life and Enhanced Low-Temperature Sodium-Ion Batteries, Advanced Energy Materials 15(11) (2025) 2403306. https://doi.org/https://doi.org/10.1002/aenm.202403306.

[9] H. Chen, K. Chen, J. Yang, B. Liu, L. Luo, H. Li, L. Chen, A. Zhao, X. Liang, J. Feng, Y. Fang, Y. Cao, Designing Advanced Electrolytes for High-Safety and Long-Lifetime Sodium-Ion Batteries via Anion–Cation Interaction Modulation, Journal of the American Chemical Society 146(23) (2024) 15751-15760. https://doi.org/10.1021/jacs.4c01395.